

OPEN ACCESS

EDITED BY

Dipesh Rupakheti,
Nanjing University of Information
Science and Technology, China

REVIEWED BY

Shazia Rehman,
Pak-Austria Fachhochschule Institute
of Applied Sciences and
Technology, Pakistan
Qiangqiang Xu,
Northwest Institute of
Eco-Environment and Resources
(CAS), China
Dongyang Yang,
Henan University, China

*CORRESPONDENCE

Peng Wang
wangpengjlu@jxnu.edu.cn

SPECIALTY SECTION

This article was submitted to
Environmental Health and Exposome,
a section of the journal
Frontiers in Public Health

RECEIVED 22 September 2022

ACCEPTED 04 November 2022

PUBLISHED 17 November 2022

CITATION

She Y, Chen Q, Ye S, Wang P, Wu B and
Zhang S (2022) Spatial-temporal
heterogeneity and driving factors of
PM_{2.5} in China: A natural and
socioeconomic perspective.
Front. Public Health 10:1051116.
doi: 10.3389/fpubh.2022.1051116

COPYRIGHT

© 2022 She, Chen, Ye, Wang, Wu and
Zhang. This is an open-access article
distributed under the terms of the
[Creative Commons Attribution License
\(CC BY\)](https://creativecommons.org/licenses/by/4.0/). The use, distribution or
reproduction in other forums is
permitted, provided the original
author(s) and the copyright owner(s)
are credited and that the original
publication in this journal is cited, in
accordance with accepted academic
practice. No use, distribution or
reproduction is permitted which does
not comply with these terms.

Spatial-temporal heterogeneity and driving factors of PM_{2.5} in China: A natural and socioeconomic perspective

Yuanyang She^{1,2}, Qingyan Chen³, Shen Ye^{1,2}, Peng Wang^{1,2*},
Bobo Wu^{1,2} and Shaoyu Zhang^{1,2}

¹School of Geography and Environment, Jiangxi Normal University, Nanchang, China, ²Key Laboratory of Poyang Lake Wetland and Watershed Research, Ministry of Education, Jiangxi Normal University, Nanchang, China, ³Science and Technology College, Jiangxi Normal University, Jiujiang, China

Background: Fine particulate matter (PM_{2.5}), one of the major atmospheric pollutants, has a significant impact on human health. However, the determinant power of natural and socioeconomic factors on the spatial-temporal variation of PM_{2.5} pollution is controversial in China.

Methods: In this study, we explored spatial-temporal characteristics and driving factors of PM_{2.5} through 252 prefecture-level cities in China from 2015 to 2019, based on the spatial autocorrelation and geographically and temporally weighted regression model (GTWR).

Results: PM_{2.5} concentrations showed a significant downward trend, with a decline rate of 3.58 μg m⁻³ a⁻¹, and a 26.49% decrease in 2019 compared to 2015, Eastern and Central China were the two regions with the highest PM_{2.5} concentrations. The driving force of socioeconomic factors on PM_{2.5} concentrations was slightly higher than that of natural factors. Population density had a positive significant driving effect on PM_{2.5} concentrations, and precipitation was the negative main driving factor. The two main driving factors (population density and precipitation) showed that the driving capability in northern region was stronger than that in southern China. North China and Central China were the regions of largest decline, and the reason for the PM_{2.5} decline might be the transition from a high environmental pollution-based industrial economy to a resource-clean high-tech economy since the implementation the Air Pollution Prevention and Control Action Plan in 2013.

Conclusion: We need to fully consider the coordinated development of population size and local environmental carrying capacity in terms of control of PM_{2.5} concentrations in the future. This research is helpful for policy-makers to understand the distribution characteristics of PM_{2.5} emission and put forward effective policy to alleviate haze pollution.

KEYWORDS

PM_{2.5}, spatial-temporal heterogeneity, natural and socioeconomic factors, driving ability, GTWR

1. Introduction

Rapid urbanization has resulted in serious air pollution, such as haze, dust and other terrible weather frequently, which bring a huge impact on people's lives, industrial and agricultural production (1–3). PM_{2.5} (particulate matter with an aerodynamic diameter $\leq 2.5 \mu\text{m}$), one of the major air pollutants, has been a popular research topic for academics in recent years (4–7). Many studies have shown that prenatal exposure of pregnant women to PM_{2.5} increases the likelihood of respiratory infection and may even cause early-life respiratory tract diseases to newborns (8), and children exposed to polluted air for a long time may increase the possibility of hypertension, asthma, obesity and metabolic disorders (9). Recent researches have also shown that high concentrations of PM_{2.5} are associated with high COVID-19 mortality (10). Thus, PM_{2.5} pollution incidents have affected human and ecological health in the course of rapid socioeconomic development.

Numerous scholars have done extensive research on PM_{2.5} in terms of components and sources, spatial variation and impact factors, and have proposed many corresponding control measures (11–16). Previous studies have shown that natural and socioeconomic factors have a significant impact on PM_{2.5} (2, 17–19). For example, the increase in temperature is conducive to atmospheric flow, which enhances PM_{2.5} dispersion, alike the higher summer temperature (lower heating energy consumption) are beneficial to the reduction of PM_{2.5} concentrations (20). On the contrary, the higher temperatures promote the formation of secondary aerosols from gas precursors, thereby increasing PM_{2.5} concentrations (21). The stronger air movement in areas with high levels of surface fine particles was likely to increase PM_{2.5} concentrations, and air movement also has a diffusion and transport effect on PM_{2.5} concentrations (22, 23). Precipitation and relative humidity played an important role in the deposition of PM_{2.5}, and increased relative humidity increases the water-soluble ion content of the air (24).

Meanwhile, some researches have shown that there was an inverted U-shaped relationship between PM_{2.5} concentrations and the economic development in socioeconomic terms (25). Extensive economic development relying on energy and resource consumption will increase pollution sources and cause deterioration of air quality. Yet, the residents will pay attention to environmental conservation and health impacts from pollutants with improving standards of living (26). The Environmental Kuznets Curve (EKC) relationship was observed between per capita GDP and air contaminant (27, 28). Industrial structure is an important indicator of local social and economic development. It is generally believed that secondary industry generally refers to heavy industrial production, which is easy

to cause greater environmental pollution. The tertiary industry mainly refers to business, finance, trust and service industries, which are generally considered to have low environmental pollution. The population density has a significant impact on PM_{2.5} emissions across all sectors (3). For instance, the increase in population density led to increased consumption, increased travel and production activities, thereby increasing PM_{2.5} emissions. However, the drivers of natural and social factors on PM_{2.5} at different spatial and temporal scales are not well understood. Therefore, it is necessary to further clarify the effects of natural and social factors on PM_{2.5} drivers at different scales.

China became the world's second-largest economy in 2010 after only 30 years of rapid economic evolution since the reform and opening up, and it has been one of the regions with the highest PM_{2.5} concentrations in the world (13). There had been many studies on the temporal and spatial distribution characteristics and influencing factors of PM_{2.5} in China (29–33). And yet, China is a country with a vast territory, a large population, complex landforms and climate, and unbalanced economic development. It poses major challenges for the research and governance of PM_{2.5}. Due to the differences in spatial-temporal scale and methods, the research results of dominant factors for spatial-temporal variation of PM_{2.5} concentrations are different. Many studies indicated that PM_{2.5} concentrations showed a spatial distribution characteristic of high overall in the north and low in the south. The pollution hotspots of PM_{2.5} were mainly concentrated in eastern and central China, especially in the Beijing-Tianjin-Hebei region and its surrounding area. The Chinese government has taken a series of strategies to control air pollution such as the Air Pollution Prevention and Control Action Plan (Action Plan) from 2013. Since the implementation of the Action Plan, PM_{2.5} concentrations have been effectively controlled and have shown a downward trend (34, 35). But there are few studies on the driving forces of the temporal and spatial variation of PM_{2.5} in China since the implementation of the Action Plan using natural and socioeconomic factors.

Therefore, it is necessary to explore the driving of natural and socioeconomic factors on PM_{2.5} concentrations in whole China. The present study focuses on the following questions by collecting the measured data of PM_{2.5}, natural and socioeconomic from 252 prefecture-level cities in China during 2015~2019: 1) The ability of natural and socioeconomic factors to drive the spatial distribution of PM_{2.5} concentrations. 2) Whether natural or social factors dominate the main causes of PM_{2.5} concentrations changes over time at different spatial scales. The result of this study may be useful to the government in the prevention and control of PM_{2.5} concentrations in industrial restructuring and population development planning.

2. Materials and methods

2.1. Study area and data source

The data in this study was primarily divided into PM_{2.5} data from 252 prefecture-level cities in China from 2015 to 2019, as well as related to urban natural and socioeconomic factors. PM_{2.5} data were obtained from hourly PM_{2.5} monitoring data by the China National Environmental Monitoring Centre (CNEMC, <http://www.cnemc.cn/>). Hourly PM_{2.5} data were compiled into the daily average data of 252 cities according to the China Ambient Air Quality Standards (GB3095-2012), the China Ambient Air Quality Assessment Technical Regulations (HJ663-2013) and other relevant regulations. Cities with multiple monitoring stations had their data averaged and treated as daily urban average data. Based on previous studies and the physical geographic features of the country, 252 cities in the country were divided into seven major zones ([Supplementary Figure S1](#) and [Supplementary Table S1](#)).

According to previous research (17, 20, 30, 36), eight main influencing factors were finally selected from the twelve factors preliminarily screened by the collinearity treatment. Natural factors include relative humidity (RH), temperature (TEMP), wind speed (WS) and precipitation (PCP), which were taken from the National Weather Science Data Centre (NWSDC). The annual-average values of RH, TEMP and WS were obtained on the average daily data. PCP was the total annual precipitation of the city. The secondary industry was selected as the driving factor of industrial structure on PM_{2.5} in the majority of previous research. With the increase of the proportion of tertiary industry, its impact on PM_{2.5} concentrations needs to be studied. Per capita GDP indicators generally represent the level of local economic development. So the socioeconomic factors included per capita GDP (GDPP), secondary industry share (SI), tertiary industry share (TI) and population density (PD) (year-end total population/total area of jurisdiction) from the China Urban Statistical Yearbook, with the missing data was interpolated by contemporaneous neighboring or around areas. The statistical description and overall spatial distribution of the eight selected driving factors from 2015 to 2019 are showed in [Table 1](#) and [Supplementary Figures S2, S3](#).

2.2. Study methods

2.2.1. Spatial autocorrelation analysis

Spatial autocorrelation analysis is a model to explore the similarity or correlation of spatial proximity observation results. Global spatial autocorrelation analysis focused on the correlation between observations in close proximity (37). Global Moran's *I* is the most widely known and used statistic to test for the presence of spatial dependence in observations. The Moran's

I can be calculated using Eq:

$$I = \frac{\sum_{i=1}^n \sum_{j=1}^n w_{ij}(x_i - \bar{x})(x_j - \bar{x})}{\frac{1}{n} \sum_{i=1}^n (x_i - \bar{x})^2 * \sum_{i=1}^n \sum_{j=1}^n w_{ij}} \quad (1)$$

where $\bar{x} = \frac{1}{n} \sum_{i=1}^n x_i$, *n* is the number of spatial units (in this study, *n* = 252); x_i and x_j are the observations of spatial units *i* and *j*, respectively; w_{ij} is an element of the spatial weight matrix *W* which describes the spatial arrangement of all the spatial units in the sample, where $w_{ij} = 1$ if spatial units *i* and *j* share a common border and $w_{ij} = 0$ otherwise. Values of Global Moran's *I* range from -1 to 1; a positive (or negative) correlation exists among the observations if $0 < I < 1$ (or $-1 < I < 0$), and the observations are distributed randomly (no correlation) in the space if *I* is close to or equals 0.

The significance of Global Moran's *I* is commonly measured by the standardized statistic *Z* as shown in Eq:

$$Z(I) = \frac{I - E(I)}{\sqrt{Var(I)}} \quad (2)$$

where *E(I)* and *Var(I)* are the expected value and variance of Moran's *I*, respectively; the methods used to calculate them are listed in the [Supplementary materials](#).

The specific location and distribution pattern of local spatial clustering were further determined by a local spatial autocorrelation. The local Moran's *I* was represented by local indicators of spatial association (LISA), which were calculated as follows:

$$LISA = \frac{(x_i - \bar{x})}{\sqrt{S^2}} \sum_j w_{ij}(x_j - \bar{x}) \quad (3)$$

$$S^2 = \frac{1}{n} \sum_{i=1}^n (x_i - \bar{x})^2 \quad (4)$$

A local spatial autocorrelation analysis can detect four cluster types with statistical significance: high-high clusters (high-incidence areas enclosed by high incidence areas); high-low clusters (high incidence areas enclosed by low-incidence areas); low-high clusters (low-incidence areas enclosed by high-incidence areas); and low-low clusters (low-incidence areas enclosed by low-incidence areas). The results were visualized in ArcGIS 10.6 software.

2.2.2. Geographically and temporally weighted regression model

The geographically and temporally weighted regression (GTWR) model (38) can effectively deal with Spatial-temporal non-stationarity by introducing a temporal dimension based on spatial heterogeneity. This model can simulate PM_{2.5} concentrations at a higher spatial resolution and accuracy across

TABLE 1 Description of the data used in this study.

Indicators	Data source	Symbol	Unit	Mean	SD	Minimum	Maximum
Relative humidity	Resource and	RH	%	68.74	10.74	29.81	99.61
Temperature	Environmental	TEMP	°C	14.43	5.31	-0.20	25.44
Wind speed	Science data	WS	m/s	2.21	0.67	0.74	6.44
Precipitation	Center	PCP	mm	1034.85	602.39	21.45	4102.50
Per capita GDP		GDPP	CNY	69110.59	36309.00	15356.00	217313.00
Secondary industry share	China City	SI	%	42.41	10.08	10.68	72.90
Tertiary Industry share	Statistical	TI	%	48.12	9.67	26.12	83.52
Population density	Yearbook	PD	person/km ²	408.73	347.95	1.66	2836.22

China than some previous models (39). The basic formula is as follows (40):

$$Y_i = \beta_0(\mu_i, v_i, t_i) + \sum \beta_k(\mu_i, v_i, t_i)X_{it} + \varepsilon_i \quad (5)$$

where (μ_i, v_i, t_i) is the spatial-temporal coordinate of the i th sample; μ_i, v_i, t_i are the longitude, latitude and time of the i th sample point, respectively; $\beta_0(\mu_i, v_i, t_i)$ denotes the regression constant at the i th sample point, i.e., the constant term in the model; X_{it} is the value of the k th independent variable at the i th point; ε_i is the residual; $\beta_k(\mu_i, v_i, t_i)$ is the k th regression parameter for the i th sample point, which is estimated as follows:

$$\hat{\beta}(\mu_i, v_i, t_i) = [X^T W(\mu_i, v_i, t_i) X]^{-1} X^T W(\mu_i, v_i, t_i) Y \quad (6)$$

where $\hat{\beta}(\mu_i, v_i, t_i)$ is the estimated value of $\beta_k(\mu_i, v_i, t_i)$; X is the matrix of independent variables; X_t is the transpose of the matrix; Y is the matrix of composition in the sample; $W(\mu_i, v_i, t_i)$ is the spatial-temporal weight matrix. W is chosen as the Gaussian distance function, the spatial-temporal weight matrix is obtained using the bi-square spatial weight function, and the spatial-temporal distance between sample i and sample j is:

$$d_{ij} = \sqrt{\delta[(U_i - \mu_j)^2 + (v_i - \mu_j)^2 + \mu(t_i - t_j)^2]} \quad (7)$$

where the choice of bandwidth affects the establishment of spatial-temporal weights, this paper adopts the Akaike Information Criterion (AICc) law for adaptive bandwidth.

2.2.3. Stability estimation of coefficients

To analyze the spatiotemporal heterogeneity of each variable, we applied the Kernel function to check the stability of the correlation coefficients, and use the coefficient distribution to observe the spatiotemporal characteristics (41). The density function of the variable x is as follows:

$$f(x) = \frac{1}{Nh} \sum_{i=1}^n k\left(\frac{x_i - \bar{x}}{h}\right) \quad (8)$$

where x_i is the coefficients subordinated to independent and identical distributions. n, h, \bar{x} represent the number of x , bandwidth and mean value, respectively. The Epanechnikov function was adopted as the kernel function for estimation in this work.

3. Results and analysis

3.1. Spatial-temporal characteristics of PM_{2.5} concentrations

The Central, East, Northwest and North China were the regions with high mean PM_{2.5} concentrations, which were 54.03 ± 13.86 , 44.71 ± 14.52 , 40.38 ± 12.55 , and $37.34 \pm 18.53 \mu\text{g m}^{-3}$, respectively, (Figures 1, 2). The mean concentrations of PM_{2.5} in southwest China was lowest ($26.50 \pm 13.41 \mu\text{g m}^{-3}$), followed by South China ($33.98 \pm 5.95 \mu\text{g m}^{-3}$). The area-weighted mean concentrations of PM_{2.5} in China from 2015 to 2019 were 44.24 ± 17.68 , 40.24 ± 15.76 , 37.54 ± 14.66 , 33.19 ± 12.60 , $32.52 \pm 13.77 \mu\text{g m}^{-3}$, respectively, and it was $37.55 \pm 15.62 \mu\text{g m}^{-3}$ in 5 years. The mean concentrations

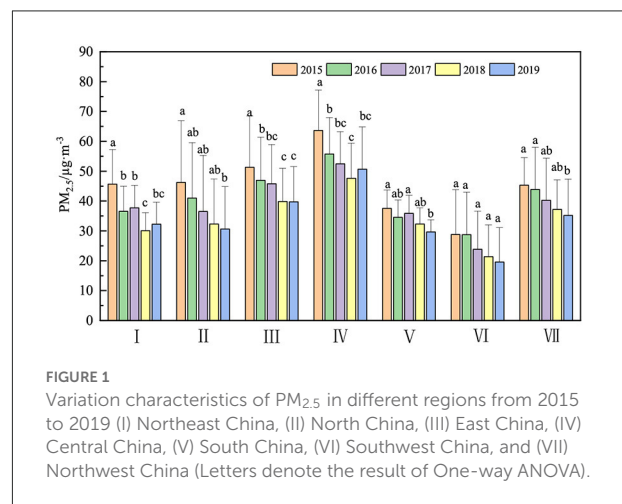
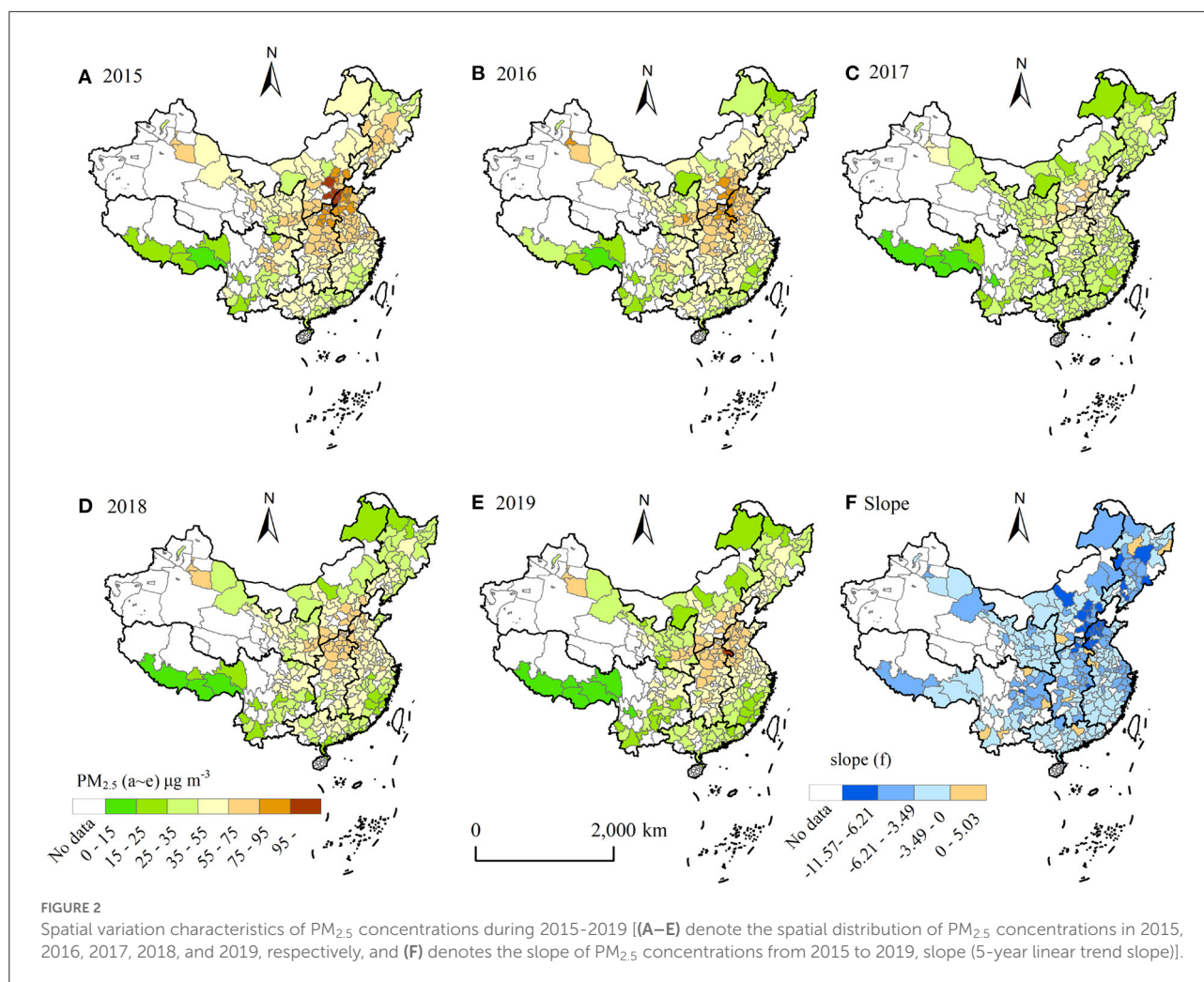


FIGURE 1 Variation characteristics of PM_{2.5} in different regions from 2015 to 2019 (I) Northeast China, (II) North China, (III) East China, (IV) Central China, (V) South China, (VI) Southwest China, and (VII) Northwest China (Letters denote the result of One-way ANOVA).



of PM_{2.5} exceeded the annual PM_{2.5} grade II standard (35 $\mu\text{g m}^{-3}$) (GB3095 2012) in 2015, 2016 and 2017, which exceeded 26.4 % in 2015, and 5.2%, 7.1% below annual PM_{2.5} grade II standard in 2018, 2019, respectively. The downward trend of PM_{2.5} concentrations was 3.58 $\mu\text{g m}^{-3}$ from 2015 to 2019, with a percentage decrease of 26.49% in 2019 compared to 2015. PM_{2.5} concentrations of 240 cities showed a decreasing trend among the 252 cities, with the proportion of decreasing cities reaching 95.24%, of which 42 cities had a decrease rate of more than 5 $\mu\text{g m}^{-3} \text{ a}^{-1}$, accounting for 16.67% of the total number of decreasing cities (Figures 1, 2). Although whole regions presented a downward trend from 2015 to 2019, PM_{2.5} concentrations exhibited an obvious spatial heterogeneity in the different regions. The largest decline occurred in North China ($-3.99 \mu\text{g m}^{-3} \text{ a}^{-1}$), followed by central China ($-3.41 \mu\text{g m}^{-3} \text{ a}^{-1}$). The region with the smallest decline was North China ($-1.80 \mu\text{g m}^{-3} \text{ a}^{-1}$). In this study, the slope of change was divided into four classes according to the natural breakpoint method [strong negative ($-11.5 \sim -6.21 \mu\text{g m}^{-3} \text{ a}^{-1}$), mid

negative ($-6.21 \sim -3.49 \mu\text{g m}^{-3} \text{ a}^{-1}$), weak negative ($-3.49 \mu\text{g m}^{-3} \text{ a}^{-1}$) and weak positive ($0 \sim 5.03 \mu\text{g m}^{-3} \text{ a}^{-1}$)]. It can be found that the strong negative area was mainly located in the Beijing-Tianjin-Hebei region and parts of the northeast, the mid negative region was mainly located in Central China and Cheng-Yu Region, East China, Northeast China and the majority of the other areas were weak negative growth regions. The weak positive area was scattered throughout the country without obvious aggregation areas (Figure 2F).

To further detect local agglomeration of PM_{2.5} concentrations, we adopted a local Moran's *I* test (Table 2). From 2015 to 2019, the average value of the global Moran's *I* was 0.57 ($p < 0.01$), indicating that PM_{2.5} concentrations showed a club convergence trend. In addition, we also calculated local Moran's *I*, the results of which revealed a detailed local pattern of spatial clustering with changes in PM_{2.5} concentrations. The Moran's *I* value showed a trend of decreasing and then increasing, with the lowest value in 2017 and the highest values in 2018

TABLE 2 Global spatial autocorrelation test.

Year	Moran'I	Z	P
2015	0.57	26.55	0.001
2016	0.56	26.17	0.001
2017	0.52	22.83	0.001
2018	0.59	27.26	0.001
2019	0.59	26.35	0.001

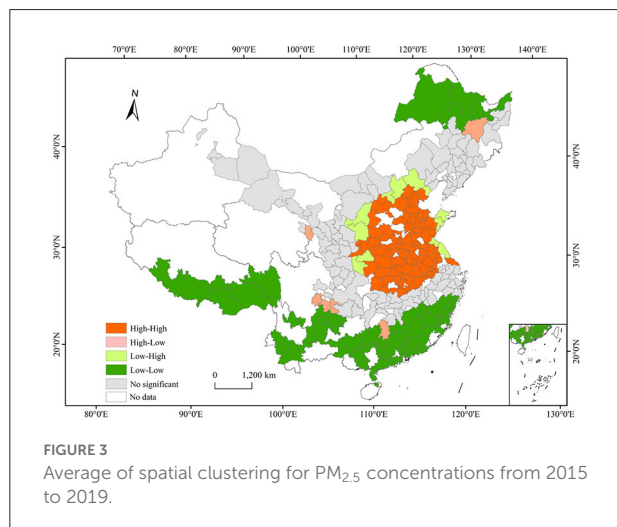


FIGURE 3
Average of spatial clustering for PM_{2.5} concentrations from 2015 to 2019.

and 2019, which indicated that an overall trend toward aggregation.

It was discovered that high-high clusters regions were primarily distributed in China's East-central region, including Beijing, Tianjin, Hebei, Shaanxi, Shanxi, Henan, Hubei, Anhui, and Shandong provinces through local spatial autocorrelation analysis. In contrast, low-low clusters were mainly located in the south and southwest provinces of China, including Tibet, Sichuan, Yunnan, Guangxi, Hainan, Guangdong, and Fujian. In addition, low and low aggregation areas also appeared in northeastern Inner Mongolia and northwestern Heilongjiang. The high-low agglomeration area and the low-high agglomeration area were small in scope and are distributed near the high-high and low-low agglomeration areas (Figure 3).

3.2. Driving forces of variation of PM_{2.5} concentrations

This study selected the GTWR model to analyze the driving forces of temporal and spatial variation of PM_{2.5} concentrations. In order to avoid the deviation of the estimation results caused

by the interaction between the indicators, eight driving factors were determined by collinearity test. The results showed that the variance inflation index of each factor was less than 10, and the condition index was also less than 30, indicating that the factor selected in this study does not have a collinear relationship (Table 3). At the same time, in order to avoid the influence of data on the magnitude, PM_{2.5} concentrations and eight driving factors were standardized before modeling. Then the temporal and spatial non-stationary relationships were modeled using the plug-in for ArcGIS 10.6 (with automatic optimal bandwidth settings) in GTWR produced by Huang et al. (38). The AICc value of the GTWR model was -2736.53. The determination coefficient (R^2) and adjustment determination coefficient (R^2_{adj}) of the GTWR model were 0.78. To evaluate the validity of GTWR results, ordinary least squares regression (OLS) was chosen to compare with geographically weighted regression (GWR), which describes the relationship between variables by building a global model, while GWR expresses the spatial non-stationarity of the relationship between variables through a local model with spatial dependence of parameters. The results showed that AICc values of the GTWR model were lower than those of the OLS and GWR models, and the R^2 was significantly higher, indicating that GTWR results were better than those of the OLS and GWR models (Table 4). The GTWR model coefficients can reflect the direction and intensity of PM_{2.5} driving capability. The positive value indicates the positive driving effect of explanatory variables on PM_{2.5} concentrations, and higher values indicate higher drive capacity, while negative coefficients indicate the opposite.

3.3. Stability analyzes of coefficients

From the Kernel distribution of coefficients of different variables (Figure 4), we can see that the coefficients of RH, TEMP, WS and PCP in natural factors were concentrated at approximately -0.01, 0.2, -0.1, and -0.7, respectively. This result indicates that the increase in WS and PCP had a opposite effect on PM_{2.5} concentrations in most cities, while the increase in TEMP had the promotion effect. Among the four socioeconomic factors we analyzed, the largest density of coefficients of PD was distributed at 0.5 (almost no negative values), which illustrates that with the increase in PD, PM_{2.5} concentrations in most cities were promoted. Simultaneously, the coefficients of SI was distributed at 0.2, indicating that the increase in SI will increase PM_{2.5} concentrations of most cities. In contrast, the coefficients of GDPP was left-distributed, and the peaks emerged at approximately -0.16, indicating that the increase of GDPP is beneficial to reduce the urban PM_{2.5} index in most cities during our study period.

TABLE 3 Co-linearity test and coefficients statistic description of variables.

Factors	Co-linearity test			GTWR coefficients statistic description				
	Standardization coefficient	Tolerances	VIF	Median	Mean	SD	Minimum	Maximum
Intercept	-	-	-	0.38	0.42	0.23	-0.22	1.43
RH	-0.04	0.60	1.68	-0.02	0.08	0.10	-0.44	0.29
TEMP	-0.01	0.31	3.22	0.00	0.26	0.31	-0.69	0.81
WS	-0.10	0.80	1.26	-0.11	0.13	0.12	-0.44	0.27
PCP	-0.30	0.41	2.44	-0.42	0.43	0.34	-3.13	0.22
GDPP	-0.19	0.66	1.51	-0.09	0.11	0.11	-0.29	0.49
SI	0.34	0.34	2.94	0.19	0.22	0.21	-1.47	0.62
TI	0.14	0.36	2.77	0.01	0.11	0.16	-0.91	0.47
PD	0.39	0.66	1.52	0.44	0.55	0.74	0.00	8.65

The mean value is the average of the absolute values of the coefficients.

TABLE 4 Result of accuracy evaluation of different model.

Model	AICc	R ²	R ² _{adj}
OLS	-1606.03	0.34	-
GWR	-2501.28	0.71	0.70
GTWR	-2736.53	0.78	0.78

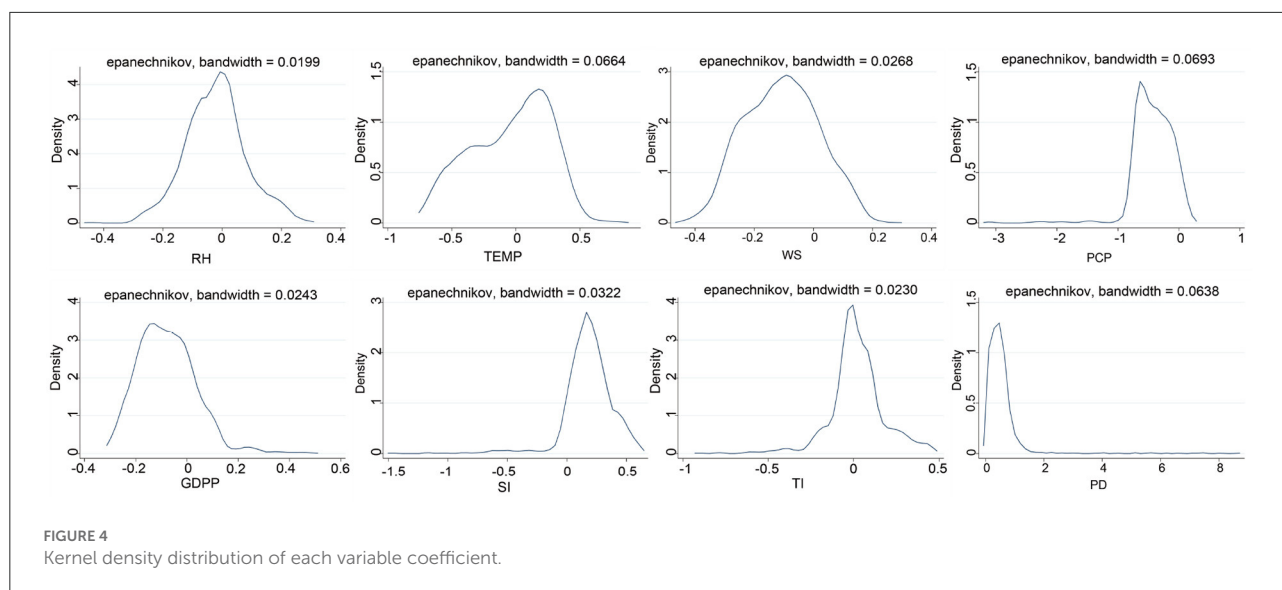
3.4. Spatial distribution characteristics of the factor driving force

The GTWR model demonstrated that the force of the driving factor presented different driving distribution characteristics in China (Figure 5). The coefficients of natural factors on PM_{2.5} concentrations were bidirectional at the national scale. RH, WS and PCP showed predominantly negative correlations. Through the analysis of the absolute value of the coefficient, influence intensity of natural factors on the regional PM_{2.5} concentrations was as follows: PCP (0.43) >TEMP (0.26) >WS (0.13) >RH (0.08). The RH coefficient was between -0.13 and 0.17. The proportion of cities with negative driving factors accounts for about 66.67% of all cities. The core region with the strongest negative impact of RH was the northeast, northwest and north China, while central China, southwest and southern China were dominated by weak positive regression coefficients. The TEMP coefficient showed positive and negative equivalence (-0.56 ~ 0.66), and positive correlation regions (48.41%) were mainly distributed in North China, Northeast China and Northwest China. The WS coefficient was mainly negative, accounting for 86.11%, and it was mainly located in the eastern, northeastern and southwestern, and the positive effect was mainly in the northwest region. The PCP coefficient of most cities (95.24%) was negative, and the high negative value area was mainly distributed in northwest and north China.

In socioeconomic factors, except that PD was positively correlated with the PM_{2.5} concentrations in each region, other factors presented a two-way impact on PM_{2.5} concentrations. The order of the absolute values of the driving factors for PM_{2.5} was PD (0.55) >SI (0.22) >GDPP (0.11) >TI (0.11). The coefficient of GDPP has a positive effect on PM_{2.5} concentrations in Southwest and Northwest China (21.03%), while North, Northeast and East China showed a negative driving relationship. The SI coefficient was mainly positive (94.05% of the total number of cities), which was negatively correlated only in the underdeveloped western region, while positively correlated in the central and eastern regions. The TI coefficient range from -0.63 to 0.26. Positively driven cities (67.46% of the total) were mainly distributed in North, Northeast and East China, but the number of cities is significantly lower than that of SI (94.05%). In particular, PD coefficient was positive throughout the region and vary considerably (0.04 to 6.93). There was an increasing trend from southeast to northwest. The lowest region was located in Guangdong and Fujian, the highest region was distributed Tibet, Inner Mongolia, Gansu and Xinjiang (Figure 5).

3.5. Temporal characteristics of driving factors

The result of the GTWR model demonstrated that the capability of driving factor was different in time scale (Figure 6). The coefficient value of the eight driving factors was between -0.50 and 0.71 in the whole region. PD (0.55) was highest average positive driving factor, followed by SI. The highest negative driving factor was PCP (-0.42), followed by WS, and the absolute values of the average coefficient of the other factors were all less than 0.05. From the analysis of the time trend, PD has the obvious downward trend (*slope* = 0.07), WS has the significantly



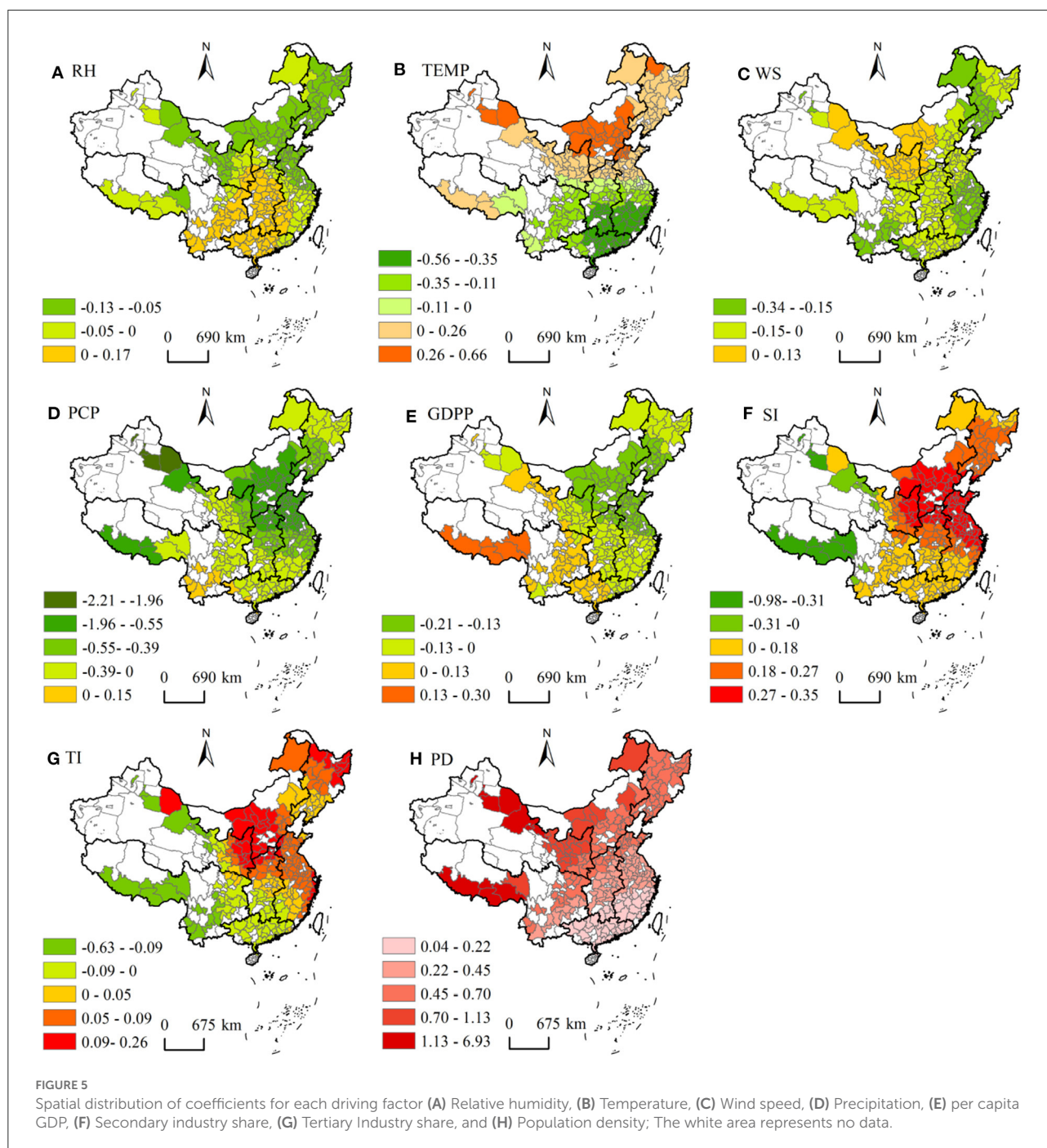
upward trend ($slope = 0.06$), and the trends in other factors were not significant ($|slope| \leq 0.04$).

From 2015 to 2019, the coefficient ranges of driving factors in Northeast and North China were $-0.77 \sim 0.75$ and $-0.76 \sim 0.91$, respectively (Figure 6). Positive driving factors of highest average value were PD (0.60, 0.67) in these two regions, followed by SI (0.22, 0.29) and TEMP (0.21, 0.32). The highest negative factor was PCP ($-0.42, -0.76$) in these two regions. Negative driving factors included WS (-0.15), GDPP (-0.14) and RH (-0.08) in Northeast China and included GDPP (-0.18) and RH (-0.07) in North China, the slope of other factors tend to be stable. From the analysis of the time change trend, the coefficient of PD and SI has obvious downward trend in Northeast China ($slope = -0.04$), PCP and WS has an upward trend ($slope = 0.13, 0.06$), and the annual trend of RH, TEMP, GDPP and SI were no obvious ($|slope| \leq 0.02$). In North China, PD and SI had obvious downward trend (both $slope = -0.04$), PCP and WS had an upward trend ($slope = 0.13, 0.06$), the annual trend of RH, TEMP, GDPP, SI were no obvious ($|slope| \leq 0.02$).

The coefficient ranges of driving factors in East, Central and South China were $-0.60 \sim 0.44$, $-0.59 \sim 0.53$ and $-0.63 \sim 0.19$ from 2015 to 2019 (Figure 6). The driving factor of the highest positive coefficient was PD (0.31, 0.37, 0.10) in the three regions, followed by SI. PCP ($-0.51, -0.47$) was the driving factor with the highest negative coefficient in East and Central China. The driving factor of the highest negative coefficient was TEMP (-0.46) in South China. The coefficients of SI and PD decreased significantly from 2015 to 2019 ($slope = -0.04, -0.03$) in East China. The coefficients of PD in Central and South China had a relatively obvious downward trend ($slope = -0.06, -0.03$). The coefficients of WS and TEMP had an obvious upward trend in East, Central and South China. The change trends of the other driving factors were no obvious ($|slope| \leq 0.03$).

The coefficient ranges of driving factors were $-0.32 \sim 0.94$ and $-0.77 \sim 1.70$ in the southwest and northwest regions from 2015 to 2019 (Figures 6G,H and Supplementary Figure S2). The driving factors of highest average positive coefficient were both PD (0.66, 1.4) in these regions, followed by GDPP (0.06) and TEMP (0.14,) respectively. The driving factor of the highest negative was PCP ($-0.15, -0.60$) in both the southwest and northwest, while other driving factors were no obvious ($|slope| \leq 0.08$). The coefficient of PD decreased significantly in the southwest and northwest from 2015 to 2019 ($slope = -0.12, -0.14$). The coefficients of TEMP and WS in the southwest region had an upward trend ($slope = 0.07$). The trends of the other driving factors were insignificant ($|slope| \leq 0.04$).

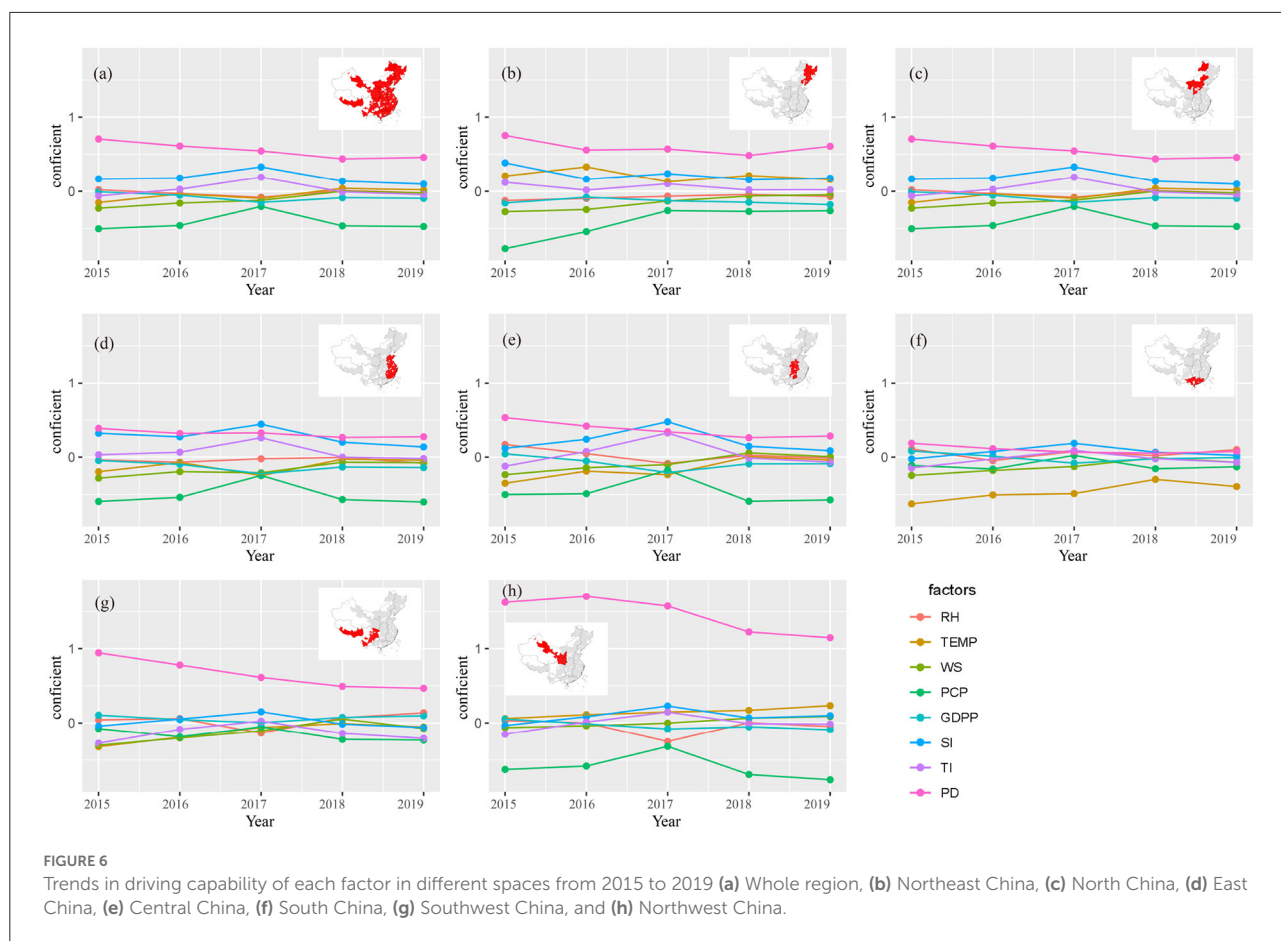
The distribution characteristics of nuclear density of each coefficient are given in Figure 7. The change of left-biased peak distribution of RH was not obvious from 2015 to 2017, and it was concentrated in positive values in 2018, whereafter the largest density of coefficients of RH was distributed at -0.4 in 2019. The temperature coefficient shown a bimodal distribution, with a main peak of about 0.3, which indicates that the rising temperature will increase the concentration of PM_{2.5} in most cities. The coefficient of PCP was left-distributed during 2015~2019, but the peak has shifted significantly to the right in 2019, indicating that the negative driving ability was weakening. The coefficient of WS showed a multi-peak distribution from 2015 to 2019, except that the peak distribution was negative in 2018. Among the four socioeconomic factors, the GDPP coefficient showed a multi-peak distribution from 2015 to 2019. The main peak was promotion effect in 2015, and then turned negative. The coefficient of SI and TI showed a multi-peak distribution from 2015 to 2019, compared with the TI, the coefficient of SI showed a right distribution, and the coefficient of TI showed a double distribution, which was close to zero,



indicating that the contribution of TI to PM_{2.5} is smaller than that of SI. The coefficients of PD had almost no negative values during 2015~2019, and had a multi-peak distribution.

Generally, among the natural factors selected in this study, except that temperature had obvious positive and negative driving effects on PM_{2.5} concentrations, the driving effects of PCP, WS and RH were mainly negative. In socioeconomic factors, GDPP and PM_{2.5} concentrations was two-way driving,

PD, SI and TI had significant positive driving effects on PM_{2.5}. The order of driving capability was PD > PCP > TEMP > SI > WS > TI > GDPP > RH. The coefficient of PD decreased most obvious in the whole study period (*slope*=-0.07), and the coefficients of SI and GDPP were decreased slightly, yet the coefficients of WS and TEMP showed an upward trend (0.06, 0.04; [Supplementary Table S3](#)). Using the global multiple regression model, a similar conclusion was reached, namely PD



(positive) and PCP (negative) were the first two drivers of PM_{2.5} concentrations ($p < 0.001$; Supplementary Table S4).

4. Discussion

This research presented that the PM_{2.5} concentrations in different areas decreased with varying degrees, with an average decrease of 3.58 μg m⁻³ a⁻¹. The series actions of energy-saving, emission-reduction and clean air proposed by the government in recent years have received some achievement. Central and East China with the higher mean PM_{2.5} concentrations have higher population densities, developed industries, intensive human activities and particulate matter emissions. The PM_{2.5} concentrations in North and central China hugely dropped may because that the developed industrial, agriculture and intensive human activities was controlled by the above actions.

Many previous studies have concluded that the severely polluted areas in China by PM_{2.5} were located in Beijing, Tianjin and Hebei and the surrounding areas (35, 42, 43). Some studies have also shown that Xinjiang has high concentrations

of PM_{2.5} in China (44–47). North China was not the region with the highest PM_{2.5} concentrations in this study because it included Inner Mongolia and other areas with relatively low PM_{2.5} concentrations. The difference of these results may be due to the spatial scale. In addition, the lack of data in parts of Xinjiang also has some impact on the overall results of the country.

We demonstrated that the capacity of driving factors was PD > PCP > TEMP > SI > WS > TI > GDPP > RH. PD was the positive main driving factor, indicating that the increase of population density will lead to the rise of PM_{2.5} concentrations. The higher population density is frequently accompanied by high emissions from household activities (e.g., cooking, heating and smoking) and local transportation (48, 49). Besides, the traffic congestion caused by population agglomeration is unfavorable for the complete combustion of motor fuel (50). In addition, the region with higher population density is often accompanied by dense buildings, which is not conducive to the diffusion of PM_{2.5}. The rational layout and design of urban buildings could promote the dispersion of pollutants and improve air quality (51), but the diffusion capacity of PM_{2.5} is rarely specified in urban building design. Exposure risk of toxic pollutants in

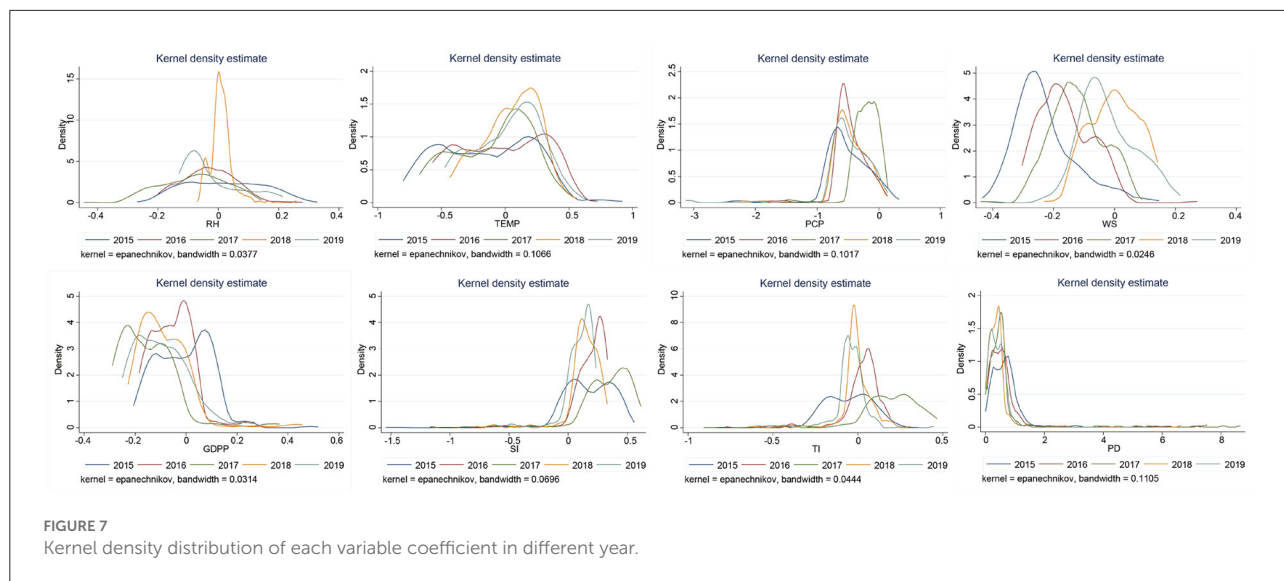


FIGURE 7 Kernel density distribution of each variable coefficient in different year.

densely populated areas is higher than that in sparsely populated areas (46). Therefore, we should pay attention to the effect of population density on PM_{2.5} concentrations.

PCP and RH were the negative main driving factors in this study, possibly because that they can enhance airborne PM_{2.5} condensation and deposition, thus reducing PM_{2.5} concentrations (52). SI had a positive driving effect on PM_{2.5} in most areas. It is well known that SI is dominated by heavy industries such as machinery, chemicals, and energy, and that it is the primary source of pollutants in the atmosphere. We found that the driving coefficient of the TI (0.11) was obvious small than that of the SI (0.22), which indicated that the TI also had a positive driving effect on PM_{2.5}, but its driving capacity was equivalent to half of that of the SI. The nonlinear relationship occurred between GDP and PM_{2.5} concentrations, such as PM_{2.5} concentrations in developed eastern regions was being controlled by advances in science and technology, as well as the optimization of industrial structure. Similar research conclusion has previously been discovered (26). Therefore, to ensure economic development while controlling pollution, the government should formulate waste emission standards, strengthen supervision and law enforcement, gradually optimize the industry, transition from SI to TI, implement strict emission standards, and compel polluting industrial enterprises to improve production capacity. Furthermore, regional industrial development should take into account the carrying capacity of the local natural environment, particularly fragile areas like the northwest.

The driving capability of PD was descending in space from northwest to southeast, which was reverse with the spatial distribution of population density. This might be because the ecological environment in Northwest China was more fragile, the environmental carrying capacity was lower, the available land

was limited, and the industrial and agricultural activities were more concentrated. This study discovered that precipitation driving capability was significantly stronger in the north than that in the south, probably because the abundant rainfall in the south and the PM_{2.5} condensed has reached the threshold. Therefore, the precipitation appears to be more important for PM_{2.5} deposition in the north of China compared to the south China, due to the little rainfall, the dry climate, and the lower vegetation cover. Similar findings have been found in previous studies, which are subject to the law of diminishing marginal effect (53, 54). The result in this study is generally consistent with the that of previous studies (55).

In this study, the region of positive driving of temperature was mainly distributed in the north China and the Qinghai-Tibet Plateau with the lower annual-average temperature. The possible reason was that the annual-average temperature in these regions was relatively lower, and the increase in temperature on the flow of the atmosphere was not enough to make PM_{2.5} diffusion, instead, promoting the flow of dry surface particulate matter. On the contrary, even though the temperature was high in the southern region, the diffusion ability was enhanced, but the small surface dust is conducive to lower the PM_{2.5} concentrations. The driving capability of WS was stronger in the north than that in the south (Figure 4), it may be caused by flat terrain in the north which provides better diffusion conditions for atmospheric pollutants, and the increase in wind speed is more conducive to the diffusion of PM_{2.5}, thereby improving regional air pollution (56). It is worth noting that WS has a stronger positive driving effect on PM_{2.5} concentrations in central and western Inner Mongolia, Xinjiang, Shaanxi, Gansu, and northeastern Sichuan. Due to these regions located on the Loess Plateau or the edge of the desert, the soil is relatively loose. When the wind speed reaches a certain level, it will also

roll up loose dust on the ground, resulting in an increase in the concentrations of PM_{2.5} in the downwind area (22). The relationship of GDPP and PM_{2.5} concentrations were negative correlation in the central and eastern regions of China, especially in the Bohai Bay economic zone. While there was a weak positive correlation in the central and western regions, indicating that pollution may decrease as per capita GDP increases (57).

The two regions with the largest decrease in PM_{2.5} concentrations were North and Central China (*slope* = -3.99 $\mu\text{g m}^{-3} \text{ a}^{-1}$, *slope* = -3.41 $\mu\text{g m}^{-3} \text{ a}^{-1}$) (Figures 1, 2). Central China was the region with the highest mean PM_{2.5} concentrations in this study, and many studies have shown that Beijing-Tianjin-Hebei in North China has always been a high-value area of PM_{2.5} in China (53, 54). The two regions are located in mid-eastern region of China and are more developed in industry and agriculture. There are slight differences (relative humidity stabilized, temperature increased slightly, and precipitation and wind speed slightly decreased) in trends of four natural factors in North China. The trend of GDPP was increased, the trends of SI and PD decreased significantly, and the trend of TI was no significant. The main negative driving factors (PCP, RH, WS) and positive driving factors (PD, SI) showed a trend of decreasing in two regions, which indicated that the decline reason of PM_{2.5} concentrations might be due to the capability weakening of the positive driving factors (PD, SI). However, trends of TEMP and WS in Central China were opposite (weakly increased in North China and weakly reduced in Central China) that in North China, and the other factors were the similar (Supplementary Figure S4), but the driving directions of TEMP and WS were different in these regions, indicating that the causes of PM_{2.5} concentrations decrease in Central and North China were similarly. This result further shows that in the case of constant or even adverse natural factors, a series of emission reduction measures introduced by the state after 2013, such as increasing green area, limiting vehicles, industrial emission purification, coal gasification in heating facilities, and industrial transformation, can alleviate or even cover up the impact of population density increase on the increase of PM_{2.5} concentrations.

Overall, this study found that the annual-average values of the main negative driving factors (PCP and RH) showed a downward trend ($-42.78\text{mm}\cdot\text{a}^{-1}$, $-0.39\%\cdot\text{a}^{-1}$), and the trends of WS and TEMP did not change significantly ($0.01\text{m}\cdot\text{s}^{-1}\cdot\text{a}^{-1}$) (Supplementary Figure S4), indicating that natural factors were not particularly favorable for driving the decrease of PM_{2.5} concentrations. Among the socioeconomic factors, except Northeast China, the trend of PD in other regions was rise, the trend of SI was decline significantly ($-1.21\%\cdot\text{a}^{-1}$), while the trend of TI was increase ($0.78\%\cdot\text{a}^{-1}$) (Supplementary Table S2). However, the positive main driving factor (PD) showed an upward trend, but the driving force of PD showed a significantly downward trend. The shift trend of industrial structure was

from the secondary industry to the tertiary industry (the driving capacity of the secondary industry was higher than that of the tertiary industry). It further demonstrated that the main reason for the decrease of PM_{2.5} concentrations may be the weakening of the driving ability of positive driving factor (PD) and the transfer from secondary industry to tertiary industry.

5. Conclusions

We comprehensively analyzed the spatial-temporal characteristic of PM_{2.5} and investigated the factors influencing PM_{2.5} concentrations by natural and socioeconomic factors in China. The results showed that 1) The mean PM_{2.5} concentrations was $37.55 \pm 15.62 \mu\text{g m}^{-3}$ during 2015-2019, the decreasing trend of PM_{2.5} concentrations was $3.58 \mu\text{g m}^{-3} \text{ a}^{-1}$, a decrease of 26.49% in 2019 compared to 2015, The regions with higher concentrations were mainly distributed in North China and South China, which were also the regions with the greatest decline in 5 years. 2) The capability of driving factors was PD >PCP >TEMP >SI >WS >TI >GDPP >RH, and the driving capability of socioeconomic factors on PM_{2.5} was slightly higher than that of natural factors. The strongest positive and negative driving factors were population density and precipitation, respectively. 3) North China and Central China were the two regions with the largest decreases in PM_{2.5} in the country from 2015 to 2019. The decrease in PM_{2.5} concentrations is primarily due to the implementation of a series of energy-saving and emission-reduction control measures after the Action Plan, such as clean air action and the adjustment of industrial structures by secondary and tertiary industries, which effectively offsets the impact of rising population density on PM_{2.5} concentrations.

The analysis above revealed that we should reduce PM_{2.5} concentration by improving socio-economic factors rather than waiting for natural factors to change. The industrial structure should be actively regulated and gradually changed from secondary to tertiary industry under the condition of ensuring stable economic growth, which is an important measure to ensure the socioeconomic effect while reducing PM_{2.5} concentrations. In the future, we must formulate a reasonable population policy so that population growth can be adapted to regional development, especially ecologically sensitive areas. In addition to we must consider environmental carrying capacity in urban planning and construction, balance population distribution, and other factors. Government departments should continue to develop and implement energy conservation and emission reduction measures in China, particularly densely populated areas, achieving win-win between economic development and environmental management.

Data availability statement

The original contributions presented in the study are included in the article/[Supplementary material](#), further inquiries can be directed to the corresponding author.

Author contributions

YS: conceptualization, methodology, writing—original draft, and writing—review and editing. QC: methodology, formal analysis, and writing—review and editing. SY: data curation, methodology, writing—original draft, and writing—review and editing. PW: methodology, investigation, writing—review and editing, and supervision. BW: investigation and writing—review and editing. SZ: writing—review and editing. All authors contributed to the article and approved the submitted version.

Funding

This work was supported by the National Natural Science Foundation of China (42167013).

References

- Canh NP, Hao W, Wongchoti U. The impact of economic and financial activities on air quality: a Chinese city perspective. *Environ Sci Pollut Res.* (2021) 28:8662–80. doi: 10.1007/s11356-020-11227-8
- Fang Z, Wu PY, Lin YN, Chang TH, Chiu Yh. Air pollution's impact on the economic, social, medical, and industrial injury environments in China. *Healthcare.* (2021) 9:261. doi: 10.3390/healthcare9030261
- Guo Q, Wang Y, Zhang Y, Yi M, Zhang T. Environmental migration effects of air pollution: micro-level evidence from China. *Environ Pollut.* (2022) 292:118263. doi: 10.1016/j.envpol.2021.118263
- Malley CS, Lefèvre EN. Measurement-based assessment of the regional contribution and drivers of reduction in annual and daily fine particulate matter impact metrics in Paris, France (2009–2018). *Atmos Environ.* (2019) 211:38–54. doi: 10.1016/j.atmosenv.2019.04.061
- Fu Z, Li R. The contributions of socioeconomic indicators to global PM_{2.5} based on the hybrid method of spatial econometric model and geographical and temporal weighted regression. *Sci Total Environ.* (2020) 703:135481. doi: 10.1016/j.scitotenv.2019.135481
- Ho CC, Chen LJ, Hwang JS. Estimating ground-level PM_{2.5} levels in Taiwan using data from air quality monitoring stations and high coverage of micro-sensors. *Environ Pollut.* (2020) 264:114810. doi: 10.1016/j.envpol.2020.114810
- Song Y, Xu T. The threshold and spatial effects of PM_{2.5} pollution on resident health: evidence from China. *Front Public Health.* (2022) 10:908042. doi: 10.3389/fpubh.2022.908042
- Jedrychowski WA, Perera FP, Spengler JD, Mroz E, Stigter L, Flak E, et al. Intrauterine exposure to fine particulate matter as a risk factor for increased susceptibility to acute broncho-pulmonary infections in early childhood. *Int J Hyg Environ Health.* (2013) 216:395–401. doi: 10.1016/j.ijheh.2012.12.014
- Kim JB, Prunicki M, Haddad F, Dant C, Sampath V, Patel R, et al. Cumulative lifetime burden of cardiovascular disease from early exposure to air pollution. *J Am Heart Assoc.* (2020) 9:e014944. doi: 10.1161/JAHA.119.014944
- Coker ES, Cavalli L, Fabrizi E, Guastella G, Lippo E, Parisi ML, et al. The effects of air pollution on COVID-19 related mortality in northern Italy. *Environ Resour Econ.* (2020) 76:611–34. doi: 10.1007/s10640-020-00486-1

Conflict of interest

The authors declare that the research was conducted in the absence of any commercial or financial relationships that could be construed as a potential conflict of interest.

Publisher's note

All claims expressed in this article are solely those of the authors and do not necessarily represent those of their affiliated organizations, or those of the publisher, the editors and the reviewers. Any product that may be evaluated in this article, or claim that may be made by its manufacturer, is not guaranteed or endorsed by the publisher.

Supplementary material

The Supplementary Material for this article can be found online at: <https://www.frontiersin.org/articles/10.3389/fpubh.2022.1051116/full#supplementary-material>

- Yang L, Hong S, He C, Huang J, Ye Z, Cai B, et al. Spatio-temporal heterogeneity of the relationships between PM_{2.5} and its determinants: a case study of Chinese cities in winter of 2020. *Front Public Health.* (2022) 10:810098. doi: 10.3389/fpubh.2022.810098
- Van Donkelaar A, Martin RV, Li C, Burnett RT. Regional estimates of chemical composition of fine particulate matter using a combined geoscience-statistical method with information from satellites, models, and monitors. *Environ Sci Technol.* (2019) 53:2595–611. doi: 10.1021/acs.est.8b06392
- Lim CH, Ryu J, Choi Y, Jeon SW, Lee WK. Understanding global PM_{2.5} concentrations and their drivers in recent decades (1998–2016). *Environ Int.* (2020) 144:106011. doi: 10.1016/j.envint.2020.106011
- Shanmuga Priyan R, Peter AE, Menon JS, George M, Shiva Nagendra S, Khare M. Vertical distribution of PM₁₀ and PM_{2.5} emission sources and chemical composition during winter period in Delhi city. *Air Quality Atmosphere Health.* (2022) 15:255–271. doi: 10.1007/s11869-021-01092-w
- Pak U, Ma J, Ryu U, Ryom K, Juhyok U, Pak K, et al. Deep learning-based PM_{2.5} prediction considering the spatiotemporal correlations: a case study of Beijing, China. *Sci Total Environ.* (2020) 699:133561. doi: 10.1016/j.scitotenv.2019.07.367
- Yu GH, Park S. Chemical characterization and source apportionment of PM_{2.5} at an urban site in Gwangju, Korea. *Atmospheric Pollut Res.* (2021) 12:101092. doi: 10.1016/j.apr.2021.101092
- Gui K, Che H, Wang Y, Wang H, Zhang L, Zhao H, et al. Satellite-derived PM_{2.5} concentration trends over Eastern China from 1998 to 2016: relationships to emissions and meteorological parameters. *Environ Pollut.* (2019) 247:1125–33. doi: 10.1016/j.envpol.2019.01.056
- Han X, Li H, Liu Q, Liu F, Arif A. Analysis of influential factors on air quality from global and local perspectives in China. *Environ Pollut.* (2019) 248:965–79. doi: 10.1016/j.envpol.2019.02.096
- Timmermans R, Kranenburg R, Manders A, Hendriks C, Segers A, Dammers E, et al. Source apportionment of PM_{2.5} across China using LOTOS-EUROS. *Atmosph Environ.* (2017) 164:370–86. doi: 10.1016/j.atmosenv.2017.06.003

20. Wang S, Liu X, Yang X, Zou B, Wang J. Spatial variations of PM_{2.5} in Chinese cities for the joint impacts of human activities and natural conditions: a global and local regression perspective. *J Cleaner Product.* (2018) 203:143–52. doi: 10.1016/j.jclepro.2018.08.249
21. Zhang R, Wang G, Guo S, Zamora ML, Ying Q, Lin Y, et al. Formation of urban fine particulate matter. *Chem Rev.* (2015) 115:3803–55. doi: 10.1021/acs.chemrev.5b00067
22. Yang X, Wang S, Zhang W, Zhan D, Li J. The impact of anthropogenic emissions and meteorological conditions on the spatial variation of ambient SO₂ concentrations: a panel study of 113 Chinese cities. *Sci Total Environ.* (2017) 584:318–28. doi: 10.1016/j.scitotenv.2016.12.145
23. Kim E, Kim BU, Kim HC, Kim S. Direct and cross impacts of upwind emission control on downwind PM_{2.5} under various NH₃ conditions in Northeast Asia. *Environ Pollut.* (2021) 268:115794. doi: 10.1016/j.envpol.2020.115794
24. Nguyen TH, Nagashima T, Doan QV. Air quality modeling study on the controlling factors of fine particulate matter (PM_{2.5}) in Hanoi: a case study in December 2010. *Atmosphere.* (2020) 11:733. doi: 10.3390/atmos11070733
25. Zhao L, Zhang X, Zhao F. The impact of high-speed rail on air quality in counties: econometric study with data from southern Beijing-Tianjin-Hebei, China. *J Clean Prod.* (2021) 278:123604. doi: 10.1016/j.jclepro.2020.123604
26. Apergis N, Ozturk I. Testing environmental Kuznets curve hypothesis in Asian countries. *Ecol Indic.* (2015) 52:16–22. doi: 10.1016/j.ecolind.2014.11.026
27. Buehn A, Farzanegan MR. Hold your breath: a new index of air pollution. *Energy Econ.* (2013) 37:104–13. doi: 10.1016/j.eneco.2013.01.011
28. Sica E, Sušnik S. Geographical dimension and environmental Kuznets curve: the case of some less investigated air pollutants. *Appl Econ Lett.* (2014) 21:1010–6. doi: 10.1080/13504851.2014.904485
29. Li G, Fang C, He S. The influence of environmental efficiency on PM_{2.5} pollution: evidence from 283 Chinese prefecture-level cities. *Sci Total Environ.* (2020) 748:141549. doi: 10.1016/j.scitotenv.2020.141549
30. Wang Y, Liu C, Wang Q, Qin Q, Ren H, Cao J. Impacts of natural and socioeconomic factors on PM_{2.5} from 2014 to 2017. *J Environ Manag.* (2021) 284:112071. doi: 10.1016/j.jenvman.2021.112071
31. Zhao S, Yin D, Yu Y, Kang S, Qin D, Dong L. PM_{2.5} and O₃ pollution during 2015–2019 over 367 Chinese cities: Spatiotemporal variations, meteorological and topographical impacts. *Environ Pollut.* (2020) 264:114694. doi: 10.1016/j.envpol.2020.114694
32. Zhao Y, Wang L, Huang T, Tao S, Liu J, Gao H, et al. Unsupervised PM_{2.5} anomalies in China induced by the COVID-19 epidemic. *Sci Total Environ.* (2021) 795:148807. doi: 10.1016/j.scitotenv.2021.148807
33. Zhou X, Strezov V, Jiang Y, Kan T, Evans T. Temporal and spatial variations of air pollution across China from 2015 to 2018. *J Environ Sci.* (2022) 112:161–9. doi: 10.1016/j.jes.2021.04.025
34. Wang Y, Gao W, Wang S, Song T, Gong Z, Ji D, et al. Contrasting trends of PM_{2.5} and surface-ozone concentrations in China from 2013 to 2017. *Natl Sci Rev.* (2020) 7:1331–9. doi: 10.1093/nsr/nwaa032
35. Shi G, Liu J, Zhong X. Spatial and temporal variations of PM_{2.5} concentrations in Chinese cities during 2015–2019. *Int J Environ Health Res.* (2021) 32:2695–707. doi: 10.1080/09603123.2021.1987394
36. Jia C, Huang W. What causes differences in PM_{2.5} concentration in China? structures are more important. *Econ Finan Lett.* (2022) 9:28–39. doi: 10.18488/29.v9i1.2936
37. Anselin L. *Spatial Econometrics: Methods and Models.* vol. 4. Springer Science & Business Media (1988).
38. Huang B, Wu B, Barry M. Geographically and temporally weighted regression for modeling spatio-temporal variation in house prices. *Int J Geograph Inf Sci.* (2010) 24:383–401. doi: 10.1080/13658810802672469
39. Guo B, Wang X, Pei L, Su Y, Zhang D, Wang Y. Identifying the spatiotemporal dynamic of PM_{2.5} concentrations at multiple scales using geographically and temporally weighted regression model across China during 2015–2018. *Sci Total Environ.* (2021) 751:141765. doi: 10.1016/j.scitotenv.2020.141765
40. Rey SJ. Spatial empirics for economic growth and convergence. *Geogr Anal.* (2001) 33:195–214. doi: 10.1111/j.1538-4632.2001.tb00444.x
41. Shi T, Zhang W, Zhou Q, Wang K. Industrial structure, urban governance and haze pollution: spatiotemporal evidence from China. *Sci Total Environ.* (2020) 742:139228. doi: 10.1016/j.scitotenv.2020.139228
42. An Z, Huang RJ, Zhang R, Tie X, Li G, Cao J, et al. Severe haze in northern China: a synergy of anthropogenic emissions and atmospheric processes. *Proc Natl Acad Sci USA.* (2019) 116:8657–66. doi: 10.1073/pnas.1900125116
43. Jiang Z, Jolleys MD, Fu TM, Palmer PI, Ma Y, Tian H, et al. Spatiotemporal and probability variations of surface PM_{2.5} over China between 2013 and 2019 and the associated changes in health risks: an integrative observation and model analysis. *Sci Total Environ.* (2020) 723:137896. doi: 10.1016/j.scitotenv.2020.137896
44. Lu D, Xu J, Yang D, Zhao J. Spatio-temporal variation and influence factors of PM_{2.5} concentrations in China from 1998 to 2014. *Atmosph Pollut Res.* (2017) 8:1151–9. doi: 10.1016/j.apr.2017.05.005
45. Yang D, Wang X, Xu J, Xu C, Lu D, Ye C, et al. Quantifying the influence of natural and socioeconomic factors and their interactive impact on PM_{2.5} pollution in China. *Environ Pollut.* (2018) 241:475–83. doi: 10.1016/j.envpol.2018.05.043
46. Chen J, Zhou C, Wang S, Hu J. Identifying the socioeconomic determinants of population exposure to particulate matter (PM_{2.5}) in China using geographically weighted regression modeling. *Environ Pollut.* (2018) 241:494–503. doi: 10.1016/j.envpol.2018.05.083
47. Guo P, Umarova AB, Luan Y. The spatiotemporal characteristics of the air pollutants in China from 2015 to 2019. *PLoS ONE.* (2020) 15:e0227469. doi: 10.1371/journal.pone.0227469
48. Li YJ, Sun Y, Zhang Q, Li X, Li M, Zhou Z, et al. Real-time chemical characterization of atmospheric particulate matter in China: a review. *Atmos Environ.* (2017) 158:270–304. doi: 10.1016/j.atmosenv.2017.02.027
49. Wang Y, Yuan Y, Wang Q, Liu C, Zhi Q, Cao J. Changes in air quality related to the control of coronavirus in China: Implications for traffic and industrial emissions. *Sci Total Environ.* (2020) 731:139133. doi: 10.1016/j.scitotenv.2020.139133
50. Wang S, Zhou C, Wang Z, Feng K, Hubacek K. The characteristics and drivers of fine particulate matter (PM_{2.5}) distribution in China. *J Cleaner Product.* (2017) 142:1800–9. doi: 10.1016/j.jclepro.2016.11.104
51. Zhang Y, Gu Z. Air quality by urban design. *Nat Geosci.* (2013) 6:506–506. doi: 10.1038/ngeo1869
52. Blanco-Becerra LC, Gáfarro-Rojas AI, Rojas-Roa NY. Influence of precipitation scavenging on the PM_{2.5}/PM₁₀ ratio at the Kennedy locality of Bogotá, Colombia. *Revista Facultad de Ingeniería Universidad de Antioquia.* (2015) 76:58–65. doi: 10.17533/udea.redin.n76a07
53. Li R, Wang Z, Cui L, Fu H, Zhang L, Kong L, et al. Air pollution characteristics in China during 2015–2016: spatiotemporal variations and key meteorological factors. *Sci Total Environ.* (2019) 648:902–15. doi: 10.1016/j.scitotenv.2018.08.181
54. Liu Q, Wu R, Zhang W, Li W, Wang S. The varying driving forces of PM_{2.5} concentrations in Chinese cities: insights from a geographically and temporally weighted regression model. *Environ Int.* (2020) 145:106168. doi: 10.1016/j.envint.2020.106168
55. Wang J, Wang S, Li S. Examining the spatially varying effects of factors on PM_{2.5} concentrations in Chinese cities using geographically weighted regression modeling. *Environ Pollut.* (2019) 248:792–803. doi: 10.1016/j.envpol.2019.02.081
56. Wang Y, Chen J, Wang Q, Qin Q, Ye J, Han Y, et al. Increased secondary aerosol contribution and possible processing on polluted winter days in China. *Environ Int.* (2019) 127:78–84. doi: 10.1016/j.envint.2019.03.021
57. Zhou C, Chen J, Wang S. Examining the effects of socioeconomic development on fine particulate matter (PM_{2.5}) in China's cities using spatial regression and the geographical detector technique. *Sci Total Environ.* (2018) 619:436–45. doi: 10.1016/j.scitotenv.2017.11.124